JACS
JOURNAL OF THE AMERICAN CHEMICAL SOCIETY

Communication

pubs.acs.org/JACS

Control of Multipolar and Orbital Order in Perovskite-like $[C(NH_2)_3]Cu_xCd_{1-x}(HCOO)_3$ Metal–Organic Frameworks

Nicole L. Evans,[†] Peter M. M. Thygesen,[†] Hanna L. B. Boström,[†] Emily M. Reynolds,[†] Ines E. Collings,[‡] Anthony E. Phillips,[§] and Andrew L. Goodwin*[,†]

[†]Department of Chemistry, Inorganic Chemistry Laboratory, University of Oxford, South Parks Road, Oxford OX1 3QR, U.K.

[‡]Laboratory of Crystallography, University of Bayreuth, D-95440 Bayreuth, Germany

[§]School of Physics and Astronomy, Queen Mary, University of London, 327 Mile End Road, London E1 4NS, U.K.

Supporting Information

ABSTRACT: We study the compositional dependence of molecular orientation (multipolar) and orbital (quadrupolar) order in the perovskite-like metal–organic frameworks $[C(NH_2)_3]Cu_xCd_{1-x}(HCOO)_3$. Upon increasing the fraction x of Jahn–Teller-active Cu^{2+}, we observe an orbital disorder/order transition and a multipolar reorientation transition, each occurring at distinct critical compositions x_o = 0.45(5) and x_m = 0.55(5). We attribute these transitions to a combination of size, charge distribution, and percolation effects. Our results establish the accessibility in formate perovskites of novel structural degrees of freedom beyond the familiar dipolar terms responsible for (anti)ferroelectric order. We discuss the implications of cooperative quadrupolar and multipolar states for the design of relaxor-like hybrid perovskites.

Some of the most important and interesting phenomena exhibited by conventional oxide perovskites arise from the coupling of ostensibly independent degrees of freedom.[1,2] In the colossal magnetoresistance manganites, for example, it is an interplay between charge localization, magnetic order, orbital order, and atom displacements that allows the conductivity to be switched on and off in response to external magnetic fields.[3−5] Likewise, the anomalous dielectric behavior of relaxor ferroelectrics arises from coupling of compositional variation with orbital and dipole orientations.[6]

Many of these same degrees of freedom are as relevant to metal–organic frameworks (MOFs) and hybrid inorganic/organic solids as they are to conventional oxide ceramics.[7,8] It is this realization that has fueled the quest for multiferroic MOFs, for example, where coupled magnetic spin and dipolar order would allow magnetic-field switching of bulk polarization.[9−14] The relevance to photovoltaic performance in hybrid organic perovskites is also clear: anomalous exciton lifetimes are now understood to emerge from a complex interplay between cooperative molecular tumbling, lattice vibrations, and polar displacements.[15−17]

In this context, the MOF community has focused almost exclusively on the cooperative behavior of *dipolar* degrees of freedom (e.g., molecular dipole orientations,[18−20] ion displacements,[21] and magnetic order[21−24]). However, MOFs also allow access to a variety of quadrupolar and higher-order multipolar ordering processes, the phenomenology of which is almost entirely unexplored.[25,26] For example, the charge distribution of guanidinium (point-group symmetry D_{3h}) is multipolar rather than dipolar (Figure 1a),[27] so molecular orientations in guanidinium-containing MOFs can be described by different states of multipolar order.[26] These states are conceptually related to the "hidden order" phases[28,29] of URu_2Si_2 and $Ga_3Gd_5O_{12}$ and often have no direct analogue in conventional oxide perovskites. A related phenomenon is the quadrupolar order associated with cooperative Jahn–Teller (JT) distortions

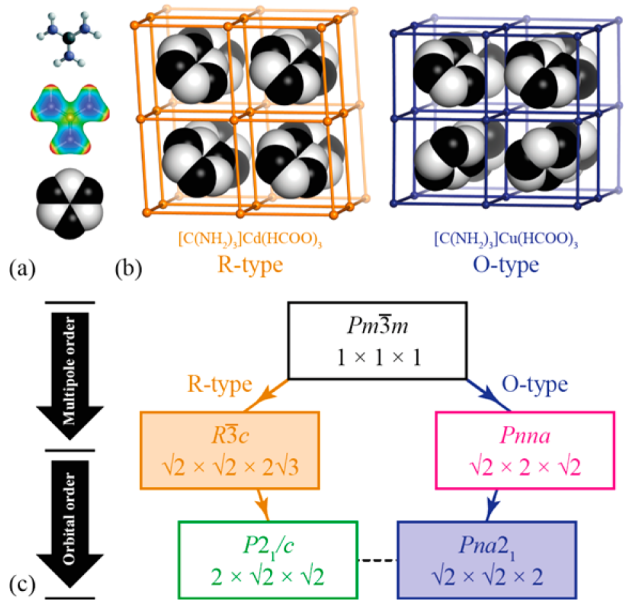

Figure 1. (a) Guanidinium ion (top), electrostatic potential (middle), and multipolar representation (bottom). (b) Multipolar order in Cd- (left) and Cu-containing (right) guanidinium formates. Metal–formate linkages are shown as straight rods. (c) Symmetry relationships between multipolar and orbital ordering processes. Arrows represent group–subgroup relationships; dashed lines represent discontinuous pathways. The space groups of the Cd (orange) and Cu (blue) formate perovskites are shaded.[30,36]

Received: May 28, 2016
Published: July 14, 2016

DOI: 10.1021/jacs.6b05208
J. Am. Chem. Soc. 2016, 138, 9393−9396

in, e.g., $[A]Cu(HCOO)_3$ hybrid frameworks (A^+ = molecular cation).[30,31] In ref 9 it was demonstrated that this quadrupolar order could itself induce a macroscopic dipole, allowing the design of polar states in a manner similar to "tilt engineering" approaches.[32] Thus, while these more complex degrees of freedom accessible to MOFs may not be directly susceptible to manipulation by external fields, they can nevertheless couple to degrees of freedom that *are* susceptible. Hence, there is substantial unrealized potential for developing new functional MOFs based on exploiting the ordering behavior of complex degrees of freedom.

Here we study the phase behavior of the hybrid perovskite analogues $[C(NH_2)_3]Cu_xCd_{1-x}(HCOO)_3$. Relatively few mixed-metal formates have been reported elsewhere,[33−35] and in this case only the x = 0 and 1 end members have been characterized previously.[30,36] They adopt structures with different guanidinium arrangements and thus are related to different states of multipolar order. Whereas in the Cd compound the molecular C_3 axes align along a single [111]-type direction of the underlying cubic net (we call this arrangement "R-type" as it enforces rhombohedral symmetry), in the Cu compound the alignment is along an alternating pair of ⟨111⟩ directions, giving an orthorhombic structure (hence "O-type") (Figure 1b). Both arrangements are mediated by hydrogen bonding between guanidinium cations and formate linkers.[30] In the absence of further distortions, the R and O multipole states have $R\bar{3}c$ and *Pnna* symmetry, respectively.[37] The lower symmetry of the Cu compound ($Pna2_1$, a polar space group) arises from coexistence of O-type multipolar order with the quadrupolar orbital order of its cooperative JT distortion.[9] Combining the same orbital arrangement with the R multipole state gives the centrosymmetric space group $P2_1/c$ [see the Supporting Information (SI)]. Hence, polarization is a nontrivial consequence of the symmetries of quadrupolar and multipolar order (Figure 1c).[9,10] By studying the Cd/Cu solid solution, we determine the extent to which the multipolar and quadrupolar order jointly responsible for bulk polarization in $[C(NH_2)_3]Cu(HCOO)_3$ might be controlled and hence exploited in future materials design.

We prepared[24,36] polycrystalline samples of $[C(NH_2)_3]Cu_xCd_{1-x}(HCOO)_3$ with x = 0, 0.1, 0.2, ..., 1; the compositions were verified using atomic absorption spectroscopy (see the SI). Synchrotron X-ray diffraction patterns show a progressive shift in peak positions and diffraction profiles consistent with solid-solution formation across the entire composition field (Figure 2a). Two clear transitions divide the phase field into three regions. The first occurs for the most Cu-poor samples ($0 \le x \le 0.4$): here the structure type is that of the Cd parent ($R\bar{3}c$), indicating R-type multipolar order and the expected absence of quadrupolar JT order. The second is observed for the single composition x = 0.5. Here the diffraction pattern can be explained by a single phase of symmetry $P2_1/c$, indicating a combination of R multipolar order and quadrupolar JT order. A monoclinic distortion is clearly evident in the splitting of relevant reflections (see the inset of Figure 2a); this splitting is not convincingly explained by a two-phase ($R\bar{3}c$ + $Pna2_1$) model (see the SI). The third and final region occurs for $0.6 \le x \le 1$, where the $Pna2_1$ phase of the Cu end member is stable. The symmetry of this phase is consistent with the same combination of O-type multipolar order and quadrupolar orbital order as in the Cu end member itself. We found no evidence for cation ordering; the crystal symmetries of each phase are consistent only with a single Cd/Cu crystallographic

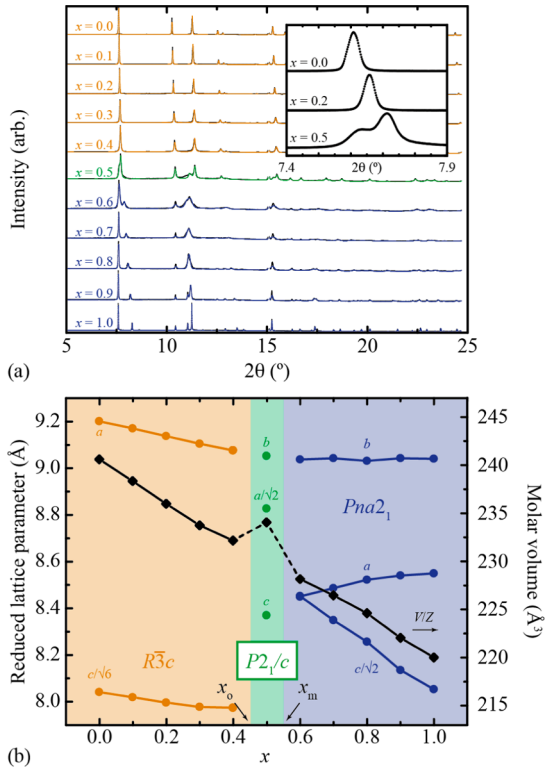

Figure 2. (a) Synchrotron X-ray diffraction patterns (λ = 0.82599(1) Å) for $[C(NH_2)_3]Cu_xCd_{1-x}(HCOO)_3$. Data are shown as black points, and Pawley fits as colored lines. The inset shows the splitting of a single reflection upon transition from $R\bar{3}c$ ($x \le 0.4$) to $P2_1/c$ (x = 0.5). (b) Corresponding lattice parameters.

site. Consequently, we attribute the transitions at x_o = 0.45(5) and x_m = 0.55(5) to orbital order and multipole reorientation transitions, respectively. To the best of our knowledge, this is the first identification of these classes of transitions in a MOF/hybrid system.

The effect of composition on the lattice parameters was determined using Pawley refinement (Figure 2b) (see the SI). Within a given phase the variation is smooth, consistent with the formation of a genuine solid solution. However, both transitions appear discontinuous and are accompanied by volume anomalies. A volume *increase* with orbital order at x_o reflects the behavior of $LaMnO_3$.[38,39] The different signs of ΔV for orbital and multipolar ordering suggests that pressure may be used to manipulate these transitions independently of one another.

How might we understand the microscopic mechanisms responsible for transitions at x_o and x_m? We suggest that increasing Cu composition has three key effects.

The first effect is that of size: the difference in the Cu−O and Cd−O bond lengths (2.1 and 2.3 Å, respectively[30,36]) means that the edge length of the cubic perovskite net is shorter in $[C(NH_2)_3]Cu(HCOO)_3$ than in $[C(NH_2)_3]Cd(HCOO)_3$ (6.03 vs 6.24 Å). This comparison holds for all of the first-row transition metals; that the analogous framework for each of these systems adopts the same O multipole state[30] suggests that this particular arrangement of guanidinium cations reflects a more efficient packing. In other words, the volume decrease upon Cu doping (Figure 2b) may drive the multipole transition in order to pack guanidinium ions more efficiently.

DOI: 10.1021/jacs.6b05208
J. Am. Chem. Soc. 2016, 138, 9393−9396

A second factor is the variation in hydrogen-bond strength between guanidinium and the framework induced as the transition metal is varied.[36,40−42] R and O multipole states should support different cation−framework interaction strengths,[41,42] suggesting that a change in charge density may also explain the transition at x_m.

The final effect we consider is that of introducing JT-active ions into a JT-inactive matrix. On one level, it is perhaps surprising that even in flexible MOFs the strains associated with JT distortions are sufficient to enforce coupling between orbital orientations of neighboring cations. However, orbital order is indisputably present in $[C(NH_2)_3]Cu(HCOO)_3$ itself.[30] For small x, the JT axes of isolated Cu^{2+} ions are uncorrelated since most are surrounded by a JT-inactive matrix of Cd^{2+}. As x increases, however, the fraction of Cu^{2+} ions with Cu^{2+} neighbors quickly increases, and strain effects enforce local coupling between orbital orientations. At some critical Cu composition these correlations become long-range, resulting in an orbital disorder/order transition; on the basis of symmetry arguments we identify this as the transition at x_o. We used a Monte Carlo simulation to identify the composition at which this transition might be anticipated (see the SI). Our toy Hamiltonian considers the effect of random-site percolation on a cubic lattice using only nearest-neighbor interactions. For this model, we find that the orbital order transition occurs at $x_o \approx 0.6$. That orbital order occurs experimentally at a lower value of x suggests that (i) there exists short-range cation order and/or (ii) JT strain fields extend beyond nearest neighbors.[43]

We investigated the temperature dependence of x_o and x_m (there is none, consistent with percolative mechanisms;[44] see the SI) and also established the corresponding phase behavior of the solid solution $[C(NH_2)_3]Mn_xCd_{1-x}(HCOO)_3$. In this JT-inactive system we observe a single temperature-dependent multipole transition from $R\bar{3}c$ directly to *Pnna* (Figure 1c) (see the SI) that occurs at a higher doping level, $x_m(Mn) = 0.75(5)$ Å, consistent with our size arguments.[45]

Therefore, we have demonstrated for a family of perovskite-like MOFs that multipolar and orbital degrees of freedom undergo independent ordering processes as a result of compositional variation. The particular system studied here has a readily identifiable signature of orbital order; however, one expects similar phenomena in, e.g., $[C(NH_2)_3]Cu_xMn_{1-x}(HCOO)_3$, where systematic absence violations would identify a progression from disordered (*Pnna*) to ordered ($Pna2_1$) states. Compositions in the vicinity of this transition may prove especially interesting since the symmetry arguments of ref 9 guarantee that critical fluctuations in orbital order must couple to fluctuations in the polarization to give polar nanodomains, as in the Pb-containing perovskite relaxors PZN/PMN.[46] Not only do our results suggest an avenue for the design of lead-free relaxors, but the inclusion of magnetic transition metals allows in principle for coupling to magnetic order. Moreover, since different organic cations have different multipolar charge distributions, substitution[47,48] is an obvious means of exploring a large variety of multipolar states. In all cases both the statistical mechanics and the symmetry implications of correlated multipolar, quadrupolar, and dipolar order will prove crucial in exploiting the degrees of freedom accessible to MOFs.

■ ASSOCIATED CONTENT

Supporting Information

The Supporting Information is available free of charge on the ACS Publications website at DOI: 10.1021/jacs.6b05208.

Experimental methods; powder diffraction refinement details; lattice parameters; Monte Carlo simulation description; symmetry discussion (PDF)

■ AUTHOR INFORMATION

Corresponding Author

*andrew.goodwin@chem.ox.ac.uk

Notes

The authors declare no competing financial interest.

■ ACKNOWLEDGMENTS

The authors gratefully acknowledge useful discussions with J. A. Hill (Oxford). The synchrotron diffraction measurements were carried out at the Diamond Light Source (I11 Beamline). We are extremely grateful for the award of a Block Allocation Grant, which made this work possible, and for the assistance in data collection provided by M. S. Senn (Oxford) and the I11 beamline staff. P.M.M.T. and A.L.G. gratefully acknowledge funding through the European Research Council (Grant 279705). I.E.C. thanks the Alexander von Humboldt Foundation for a Postdoctoral Fellowship. This project received funding from the European Union (EU) Horizon 2020 Research and Innovation Programme under Marie Sklodowska-Curie Grant Agreement 641887 (project acronym DEFNET).

■ REFERENCES

(1) Lee, J. H.; Fang, L.; Vlahos, E.; Ke, X.; Jung, Y. W.; Kourkoutis, L. F.; Kim, J.-W.; Ryan, P. J.; Heeg, T.; Roeckerath, M.; Goian, V.; Bernhagen, M.; Uecker, R.; Hammel, P. C.; Rabe, K. M.; Kamba, S.; Schubert, J.; Freeland, J. W.; Muller, D. A.; Fennie, C. J.; Schiffer, P.; Gopalan, V.; Johnston-Halperin, E.; Schlom, D. G. *Nature* **2010**, *466*, 954−959.

(2) Millis, A. J. *Nature* **1998**, *392*, 147−150.

(3) Jin, S.; Tiefel, T. H.; McCormack, M.; Fastnacht, R. A.; Ramesh, R.; Chen, L. H. *Science* **1994**, *264*, 413−415.

(4) Goodenough, J. B. *Phys. Rev.* **1955**, *100*, 564−573.

(5) Adams, C. P.; Lynn, J. W.; Mukovskii, Y. M.; Arsenov, A. A.; Shulyatev, D. A. *Phys. Rev. Lett.* **2000**, *85*, 3954−3957.

(6) Xu, G.; Zhong, Z.; Bing, Y.; Ye, Z.-G.; Shirane, G. *Nat. Mater.* **2006**, *5*, 134−140.

(7) Jain, P.; Dalal, N. S.; Toby, B. H.; Kroto, H. W.; Cheetham, A. K. *J. Am. Chem. Soc.* **2008**, *130*, 10450−10451.

(8) Rogez, G.; Viart, N.; Drillon, M. *Angew. Chem., Int. Ed.* **2010**, *49*, 1921−1923.

(9) Stroppa, A.; Jain, P.; Barone, P.; Marsman, M.; Perez-Mato, J. M.; Cheetham, A. K.; Kroto, H. W.; Picozzi, S. *Angew. Chem., Int. Ed.* **2011**, *50*, 5847−5850.

(10) Stroppa, A.; Barone, P.; Jain, P.; Perez-Mato, J. M.; Picozzi, S. *Adv. Mater.* **2013**, *25*, 2284−2290.

(11) Wang, W.; Yan, L.-Q.; Cong, J.-Z.; Zhao, Y.-L.; Wang, F.; Shen, S.-P.; Zou, T.; Zhang, D.; Wang, S.-G.; Han, X.-F.; Sun, Y. *Sci. Rep.* **2013**, *3*, 2024.

(12) Tian, Y.; Stroppa, A.; Chai, Y.; Yan, L.; Wang, S.; Barone, P.; Picozzi, S.; Sun, Y. *Sci. Rep.* **2014**, *4*, 6062.

(13) Jain, P.; Ramachandran, V.; Clark, R. J.; Zhou, H. D.; Toby, B. H.; Dalal, N. S.; Kroto, H. W.; Cheetham, A. K. *J. Am. Chem. Soc.* **2009**, *131*, 13625−13627.

(14) Gómez-Aguirre, L. C.; Pato-Doldán, B.; Mira, J.; Castro-García, S.; Señaris-Rodríguez, M. A.; Sánchez-Andújar, M.; Singleton, J.; Zapf, V. S. *J. Am. Chem. Soc.* **2016**, *138*, 1122−1125.

DOI: 10.1021/jacs.6b05208
J. Am. Chem. Soc. 2016, 138, 9393−9396

(15) Lee, J.-H.; Bristowe, N. C.; Bristowe, P. D.; Cheetham, A. K. *Chem. Commun.* **2015**, *51*, 6434−6437.
(16) Frost, J. M.; Walsh, A. *Acc. Chem. Res.* **2016**, *49*, 528−535.
(17) Leguy, A. M. A.; Frost, J. M.; McMahon, A. P.; Sakai, V. G.; Kockelmann, W.; Law, C.; Li, X.; Foglia, F.; Walsh, A.; O'Regan, B. C.; Nelson, J.; Cabral, J. T.; Barnes, P. R. F. *Nat. Commun.* **2015**, *6*, 7124.
(18) Sánchez-Andújar, M.; Presedo, S.; Yáñez-Vilar, S.; Castro-García, S.; Shamir, J.; Señarís-Rodríguez, M. A. *Inorg. Chem.* **2010**, *49*, 1510−1516.
(19) Besara, T.; Jain, P.; Dalal, N. S.; Kuhns, P. L.; Reyes, A. P.; Kroto, H. W.; Cheetham, A. K. *Proc. Natl. Acad. Sci. U. S. A.* **2011**, *108*, 6828−6832.
(20) Mączka, M.; Costa, N. L. M.; Gągor, A.; Paraguassu, W.; Sieradzki, A.; Hanuza, J. *Phys. Chem. Chem. Phys.* **2016**, *18*, 13993−14000.
(21) Xu, G.-C.; Zhang, W.; Ma, X.-M.; Chen, Y.-H.; Zhang, L.; Cai, H.-L.; Wang, Z.-M.; Xiong, R.-G.; Gao, S. *J. Am. Chem. Soc.* **2011**, *133*, 14948−14951.
(22) Saines, P. J.; Tan, J.-C.; Yeung, H. H.-M.; Barton, P. T.; Cheetham, A. K. *Dalton Trans.* **2012**, *41*, 8585−8593.
(23) Saines, P. J.; Paddison, J. A. M.; Thygesen, P. M. M.; Tucker, M. G. *Mater. Horiz.* **2015**, *2*, 528−535.
(24) Wang, Z.; Zhang, B.; Otsuka, T.; Inoue, K.; Kobayashi, H.; Kurmoo, M. *Dalton Trans.* **2004**, 2209−2216.
(25) Li, W.; Zhang, Z.; Bithell, E. G.; Batsanov, A. S.; Barton, P. T.; Saines, P. J.; Jain, P.; Howard, C. J.; Carpenter, M. A.; Cheetham, A. K. *Acta Mater.* **2013**, *61*, 4928−4938.
(26) Hill, J. A.; Thompson, A. L.; Goodwin, A. L. *J. Am. Chem. Soc.* **2016**, *138*, 5886−5896.
(27) Davis, M. R.; Dougherty, D. A. *Phys. Chem. Chem. Phys.* **2015**, *17*, 29262−29270.
(28) Mydosh, J. A.; Oppeneer, P. M. *Rev. Mod. Phys.* **2011**, *83*, 1301−1322.
(29) Paddison, J. A. M.; Jacobsen, H.; Petrenko, O. A.; Fernández-Díaz, M. T.; Deen, P. P.; Goodwin, A. L. *Science* **2015**, *350*, 179−181.
(30) Hu, K.-L.; Kurmoo, M.; Wang, Z.; Gao, S. *Chem. - Eur. J.* **2009**, *15*, 12050−12064.
(31) Wang, B.-Q.; Yan, H.-B.; Huang, Z.-Q.; Zhang, Z. *Acta Crystallogr., Sect. C: Cryst. Struct. Commun.* **2013**, *69*, 616−619.
(32) Pitcher, M. J.; Mandal, P.; Dyer, M. S.; Alaria, J.; Borisov, P.; Niu, H.; Claridge, J. B.; Rosseinsky, M. J. *Science* **2015**, *347*, 420−424.
(33) Shang, R.; Sun, X.; Wang, Z.-M.; Gao, S. *Chem. - Asian J.* **2012**, *7*, 1697−1707.
(34) Mączka, M.; Sieradzki, A.; Bondzior, B.; Deren, P.; Hanuza, J.; Hermanowicz, K. *J. Mater. Chem. C* **2015**, *3*, 9337−9345.
(35) Mączka, M.; Gagor, A.; Hermanowicz, K.; Sieradzki, A.; Macalik, L.; Pikul, A. *J. Solid State Chem.* **2016**, *237*, 150−158.
(36) Collings, I. E.; Hill, J. A.; Cairns, A. B.; Cooper, R. I.; Thompson, A. L.; Parker, J. E.; Tang, C. C.; Goodwin, A. L. *Dalton Trans.* **2016**, *45*, 4169−4178.
(37) We note that the tilt systems active in both compounds correspond to symmetries that are supergroups of the symmetries arising from multipolar order, allowing multipole−tilt coupling.
(38) Chatterji, T.; Fauth, F.; Ouladdiaf, B.; Mandal, P.; Ghosh, B. *Phys. Rev. B: Condens. Matter Mater. Phys.* **2003**, *68*, 052406.
(39) Ahmed, M. R.; Gehring, G. A. *Phys. Rev. B: Condens. Matter Mater. Phys.* **2009**, *79*, 174106.
(40) Li, W.; Thirumurugan, A.; Barton, P. T.; Lin, Z.; Henke, S.; Yeung, H. H.-M.; Wharmby, M. T.; Bithell, E. G.; Howard, C. J.; Cheetham, A. K. *J. Am. Chem. Soc.* **2014**, *136*, 7801−8704.
(41) Di Sante, D.; Stroppa, A.; Jain, P.; Picozzi, S. *J. Am. Chem. Soc.* **2013**, *135*, 18126−18130.
(42) Shang, R.; Xu, G.-C.; Wang, Z.-M.; Gao, S. *Chem. - Eur. J.* **2014**, *20*, 1146−1158.
(43) There is clear evidence of significant strain broadening in the diffraction patterns shown in Figure 2a that appears to be more significant for $0.6 \leq x \leq 1$ (Cd^{2+} embedded in a Cu^{2+} matrix) than for $0 \leq x \leq 0.4$ (Cu^{2+} embedded in a Cd^{2+} matrix).
(44) Whereas in conventional orbital order/disorder systems (e.g., $La_{1-x}Ca_xMnO_3$) thermally induced orbital reorganization is permitted via charge redistribution,[49] here it is likely that the distribution of JT-active cations is fixed during synthesis, resulting in the temperature independence of x_o.
(45) Shannon, R. D. *Acta Crystallogr., Sect. A: Cryst. Phys., Diffr., Theor. Gen. Crystallogr.* **1976**, *32*, 751−767.
(46) Paściak, M.; Welberry, T. R.; Kulda, J.; Kempa, M.; Hlinka, J. *Phys. Rev. B: Condens. Matter Mater. Phys.* **2012**, *85*, 224109.
(47) Kieslich, G.; Kumagai, S.; Forse, A. C.; Sun, S.; Henke, S.; Yamashita, M.; Grey, C. P.; Cheetham, A. K. *Chem. Sci.* **2016**, DOI: 10.1039/C6SC01247G.
(48) Chen, S.; Shang, R.; Wang, B.-W.; Wang, Z.-M.; Gao, S. *Angew. Chem., Int. Ed.* **2015**, *54*, 11093−11096.
(49) Rao, C. N. R.; Cheetham, A. K. *Science* **1996**, *272*, 369−370.

DOI: 10.1021/jacs.6b05208
J. Am. Chem. Soc. 2016, 138, 9393−9396